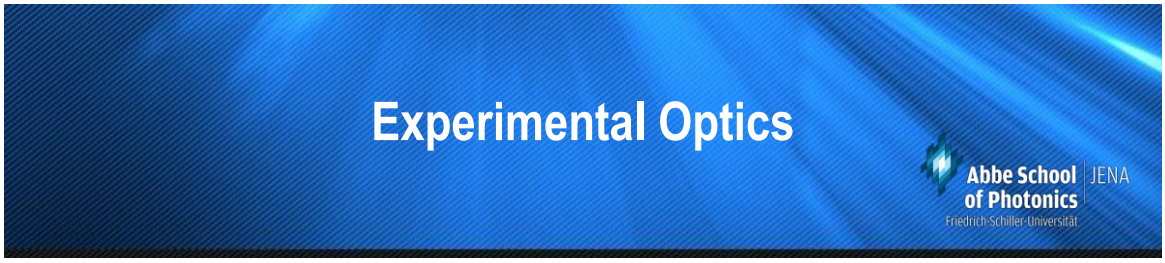

Contact:
Davide Cammi, e-mail: davide.cammi@uni-jena.de
Peter Rentschler, e-mail: peter.rentschler@gmx.de
Last edition: Davide Cammi, October 2013

Fabry-Perot Interferometer

Contents

1 Overview

The Fabry-Pérot interferometer was invented in 1897 by Charles Fabry and Alfred Pérot. In contrast to other, more conventional types like the Michelson or Mach-Zehnder interferometer, the Fabry-Pérot arrangement acts as an optical resonator which may result in an extremely high spectral resolving power $\lambda/\Delta\lambda$ up to $\sim 10^7$ for optical wavelengths λ. In this way, state-of-the-art Fabry-Pérot cavities may exceed the resolution of classical diffraction gratings by a factor of ~ 100 and provide an irreplaceable tool in particular for studies of the hyperfine structure in atomic spectra.

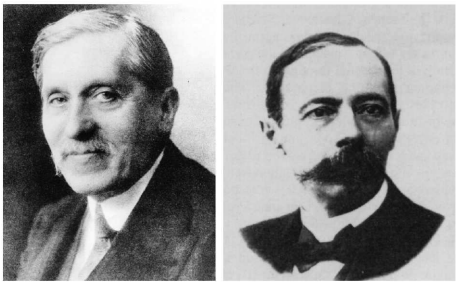

Figure 1: *Charles Fabry (1867-1945), left, and Alfred Perot (1863-1925), right, were the first French physicists to construct an optical cavity for interferometry. Figure is taken from* `http://photonics.usask.ca/photos`.

2 Safety Issues

2.1 Eye hazard

The HeNe laser used in this lab provides a cw output of 2.5 mW. Please, use appropriate **laser safety goggles** in order to avoid damage to your eyes. It is recommended to discard any reflecting accessories like watches and jewelry. Do not look directly into the laser beam. Use the key switch at the laser power supply due to **high voltage risks (20 kV)**.

2.2 Electrical hazard

The **piezo actuator** is operated at 150 V, its power supply may cause an electric shock. Do not remove the associated BNC cable from the back of the control unit PTC 1000!

3 Theoretical Background

Fabry-Pérot cavities make use of curved and plane mirrors as well, depending on their field of application. Whereas spherical mirrors are commonly employed for confocal schemes especially, the very basics of optical resonators are better studied by means of elementary plane surface reflections. We thus start with a brief description of that case and switch over afterwards to peculiarities of confocal cavities.

3.1 The plane mirror resonator

We consider two plane mirrors with equal reflectivities $0 < R < 1$ in a parallel arrangement separated by a distance d from each other. A plane wave with an amplitude $\mathbf{E}_e$ falls onto a mirror with an angle of incidence α. At each mirror surface, the beam is partially reflected (amplitude coefficient $r < 1$) and transmitted. The scheme is sketched in Fig. 2. The phase

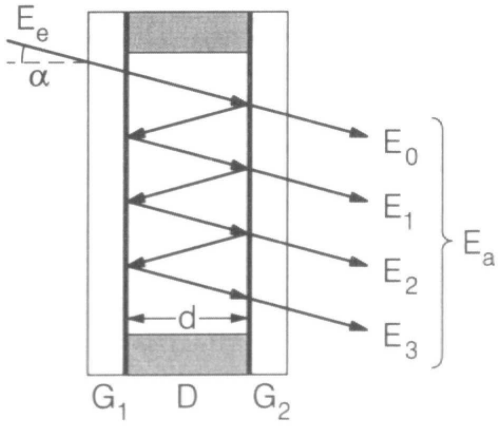

Figure 2: *Multiple-beam interference at two parallel surfaces G_1 and G_2, separated by a distance d and filled with a dielectric medium D. Figure is taken from* `http://www.loitz79.de/Physik Praktikum/Interferometrie.htm`.

difference $\Delta\phi$ between two adjacent beams E_i and E_{i+1} depends on the mirror distance d and the refractive index n of the dielectric medium:

$$\Delta\phi = \frac{4\pi}{\lambda} n\, d \cos\alpha. \tag{1}$$

We assume $n = 1$ for an air-filled resonator from now on. The output may be written as the coherent superposition of all amplitudes E_i with $0 \leq i < \infty$, since an effectively infinite number of interfering waves is assumed for mirror reflectivities near 1. The total transmitted

amplitude E_a results as

$$E_a = \sum_{n=0}^{\infty} E_n = t^2 E_e \sum_{n=0}^{\infty} r^{2n}\, e^{-in\Delta\phi} = \frac{t^2 E_e}{1 - r^2 e^{-i\Delta\phi}}, \tag{2}$$

where the initial amplitude E_e is transmitted twice: $E_0 = t^2 E_e$. We use the relations $T = t^2$ and $R = r^2$ for the intensity transmission and reflection, respectively. If there is no absorption, we have $T + R = 1$ and the transmitted intensity is given as:

$$I_T = I_e \frac{(1-R)^2}{(1-R)^2 + 4R\sin^2(\Delta\phi/2)}, \tag{3}$$

for an incident intensity $I_e \propto |E_e|^2$. Obviously, the phase difference (1) determines the transmitted wavelengths λ_m in the m^{th} order:

$$m\lambda_m = 2d \quad \text{with} \quad m \geq 1, \tag{4}$$

for an incidence angle $\alpha \to 0$. This condition defines an optical resonator, tuned by an adjustable mirror distance d. We may write Eq. (3) in an alternative form:

$$I_T = \frac{1}{1 + (2/\pi)^2 \mathcal{F}_R^2 \sin^2(\Delta\phi/2)} \quad \text{with} \quad \mathcal{F}_R \equiv \pi \frac{\sqrt{R}}{1-R}, \tag{5}$$

normalized to the incident intensity I_e. This function is plotted in Fig. 3.

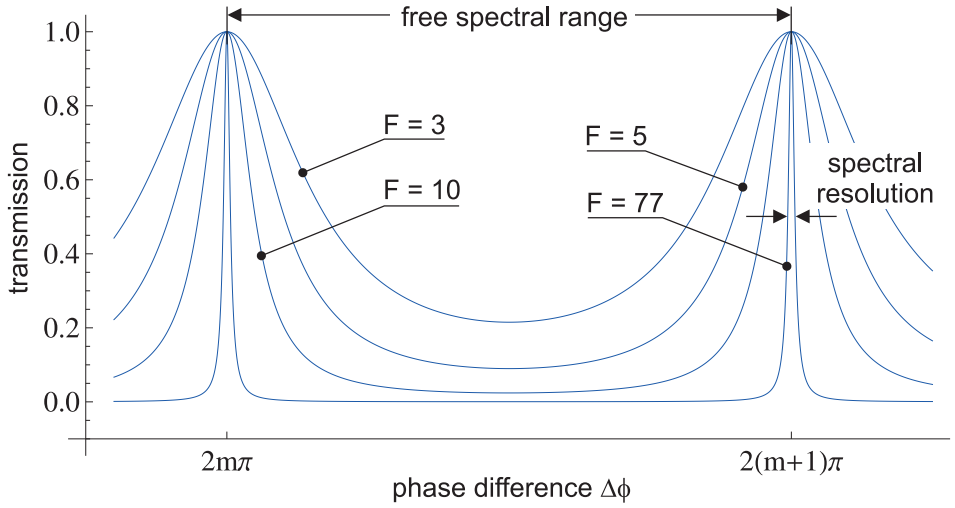

Figure 3: *Normalized transmission of a Fabry-Pérot resonator for various values of the finesse $\mathcal{F} \leq 77$ as a function of the phase difference $\Delta\phi$. A monochromatic light source is presumed.*

The *finesse* $\mathcal{F}_R$ quantifies the optical quality of the resonator made of perfectly polished and adjusted plane mirrors. However, even well-aligned resonators with plane mirrors are severely restricted to $\mathcal{F} \lesssim 50$ unless high-precision mirrors are used. The contribution of mirror irregularities which cause unwanted phase shifts at each reflection may be denoted by $\mathcal{F}_q$. An elementary theory of these surface imperfections is discussed in Appendix A. From an experimental point of view, the finesse describes the ratio between the free spectral range (FSR) $\delta\nu$ and the spectral resolution $\Delta\nu$ of the instrument in the frequency domain:

$$\mathcal{F} \equiv \delta\nu/\Delta\nu \quad \text{with} \quad \delta\nu \leq c/(2d), \tag{6}$$

where c denotes the vacuum velocity of light and the equality $\delta\nu = c/(2d)$ holds for plane mirrors. $\Delta\nu$ is usually defined as the full width (FWHM) of the resonance. The finesse $\mathcal{F}$ also indicates the effective number of interfering beams within the cavity.

Since all light rays slightly diverge from their source due to the limited spatial coherence, plane-mirror cavities always produce concentric ("Haidinger") interference rings rather than single on-axis spots. Such rings are shown on the left of Fig. 4. From their radial intensity

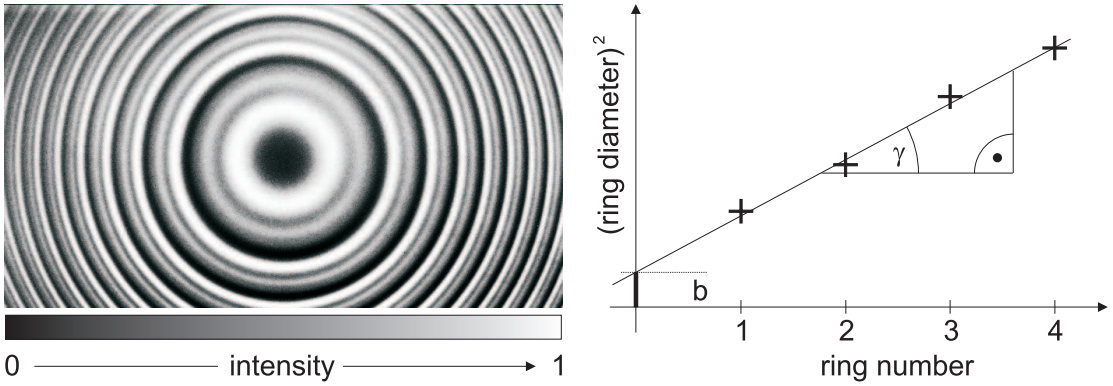

Figure 4: *Concentric interference rings of a Fabry-Pérot cavity with plane mirrors for two closely spaced spectral lines (left) and the functional dependence of the squared diameters on the ring number (right). The left figure is taken from* `http://commons.wikimedia.org`.

distribution, characteristic parameters of the setup may be obtained [2]. Following Fig. 2, the condition

$$2d\cos\left(\alpha_p\right) = m\lambda \quad \text{with} \quad p = 1, 2, 3, ... \tag{7}$$

yields interference maxima for certain incidence angles α_p and integer numbers of m. Let the innermost ring be denoted by the index "0". Obviously, we get from Equation (7):

$$2d\cos\left(\alpha_p\right) - 2d\cos\left(\alpha_0\right) = (m - m_0)\,\lambda. \tag{8}$$

The parallel transmitted light is focused to the image plane by a lens with a focal length f.

Thus, we get the diameter D_p of the p^{th} interference ring in the paraxial approximation:

$$D_p = 2f\tan\left(\alpha_p\right) \approx 2f\alpha_p \quad \text{for} \quad \alpha_p \to 0. \tag{9}$$

Combining the Equations (8) and (9), we get a linear dependence of the squared diameter D_p^2 on the ring number p:

$$D_p^2 = 4f^2\frac{\lambda}{d}(p+\varepsilon) \quad \text{with} \quad \varepsilon \equiv \alpha_0^2\frac{d}{\lambda}. \tag{10}$$

The quantity $0 \leq \varepsilon < 1$ is called the "excess" and determines the axis intercept b on the right in Figure 4. On the other hand, the slope $\tan\gamma$ of the function (10) yields the ratio λ/d.

3.2 The confocal resonator

The finesse as defined in (5) is valid for a *constant* cavity spacing d across its lateral dimensions. On-axis beams would thus receive the same optical path length as parallel off-axis rays when propagating through the resonator. In contrast, easily aligned confocal arrangements as shown on the left of Fig. 5 are made of spherical mirrors and cause various path lengths depending on the distance of the ray from the optical axis. Beams which enter the

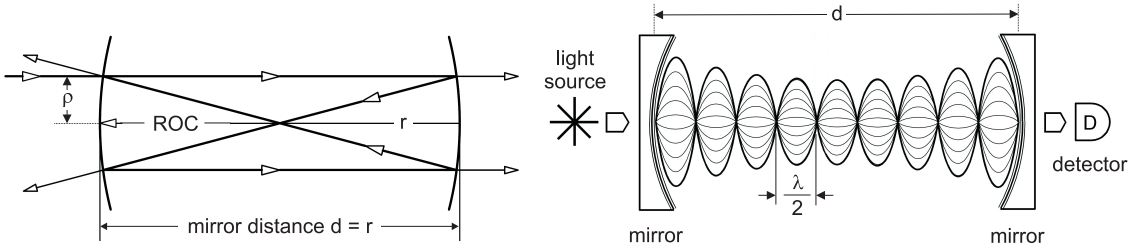

Figure 5: *Left: Geometry of confocal cavities made of two identical spherical mirrors. The mirror distance d equals to the radius of curvature r. The parallel input beam is effectively transmitted without divergence. Figure is taken from [5]. Right: Amplitude of the electric field within the confocal resonator in the case of resonance. Figure is taken from* `http://www.nano.physik.uni-muenchen.de`.

confocal cavity with an off-axis parameter $\varrho > 0$ would experience an optical path difference of $\varrho^4/4r^3$, where the radius of curvature is denoted by r [1].

A general expression for the total finesse $\mathcal{F}_t$ of confocal cavities may be thus written as

$$\frac{1}{\mathcal{F}_t} = \sqrt{\left(\frac{1}{\mathcal{F}_R}\right)^2 + \left(\frac{1}{\mathcal{F}_q}\right)^2 + \left(\frac{1}{\mathcal{F}_i}\right)^2} \quad \text{with} \quad \mathcal{F}_q \to \infty \quad \text{and} \quad \mathcal{F}_i = \frac{\lambda}{4}\frac{4r^3}{\varrho^4}, \tag{11}$$

where mirror irregularities ($\mathcal{F}_q$) have been neglected. Obviously, the reflective term $\mathcal{F}_R$

limits the total finesse for perfectly aligned resonators and on-axis rays: $\mathcal{F}_t \leq \mathcal{F}_R$. Figure 5 (right) gives an imagination of the electric field amplitude within the resonator. Note the strong field enhancement due to multiple back and forth reflections.

A more detailed analysis considers the mode spectrum inside of the cavity. Following [2], the spatial amplitude function can be written by means of the Hermitian polynomials H_n as

$$A_{mn}(\vec{r}) \propto H_m\left(\sqrt{2}w^{-1}x\right) H_n\left(\sqrt{2}w^{-1}y\right) e^{-(\rho/w)^2 - i\phi(\vec{r})} \quad \text{with} \quad m,n \,\epsilon\, \mathbb{N}_0, \tag{12}$$

where the Gaussian beam width $w(z)$ is given as $w^2(z) = w_0^2\left(1 + (2z/d)^2\right)$ with $w_0^2 = \lambda d/2\pi$. The polar coordinates are defined as $\vec{r} \equiv (\rho\cos\theta, \rho\sin\theta, z)$, assuming the origin $\vec{r} = 0$ in the center of the cavity. Obviously, the Rayleigh length $z_0 = \pm\pi w_0^2/\lambda$ coincides with the axial mirror position $\pm d/2$. Using $\xi_0 \equiv 2z_0/r$, the phase function in (12) is in general given as

$$\phi(\vec{r}) = \frac{2\pi}{\lambda} r\left[\frac{1}{2}(1+\xi_0) + \left(\frac{\rho}{r}\right)^2 \frac{\xi_0}{1+\xi_0^2}\right] - (1+m+n)\left[\frac{\pi}{2} - \arctan\left(\frac{1-\xi_0}{1+\xi_0}\right)\right]. \tag{13}$$

In case of resonance, $\phi(\vec{r}) = q\pi$ with $q \,\epsilon\, \mathbb{N}$ is required. Since r equals the mirror distance d and $\xi_0 = 1$, we find on the optical axis ($\rho = 0$) the eigenfrequencies from $c = \lambda\,\nu_{qmn}$,

$$\nu_{qmn} = \frac{c}{2d}\left[q + \frac{1}{2}(m+n+1)\right] \quad \text{such that} \quad \delta\nu = \frac{c}{4d} \quad \text{for} \quad 2q+m+n+1 \,\epsilon\, \mathbb{N}, \tag{14}$$

in contrast to plane mirror cavities which are characterized by the twofold free spectral range, as described by Eq. (6). It should be noted that the values ν_{qmn} from Eq. (14) are degenerated, since the numbers q, m, n are not unique. Fig. 6 illustrates some modes.

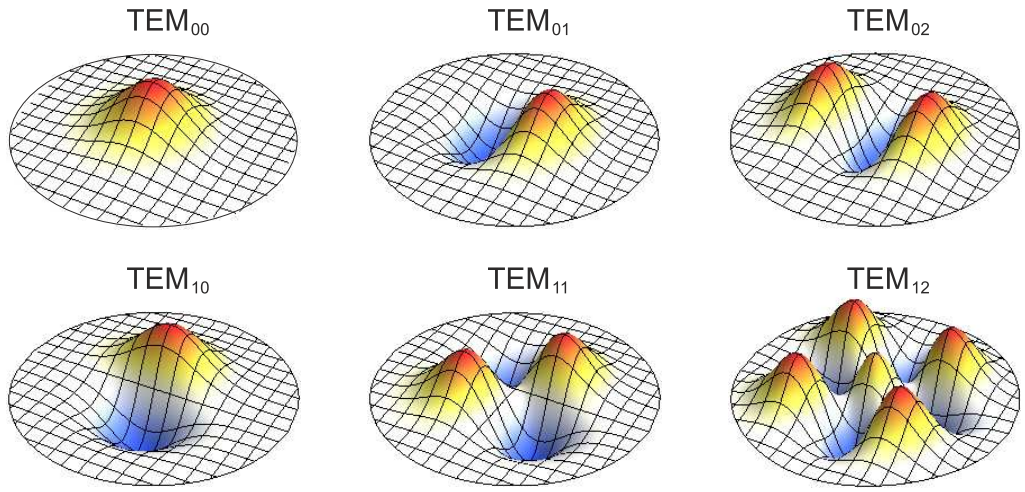

Figure 6: *Amplitude distributions $A_{mn}(\vec{r})$ in the cavity center, i.e. $z = 0$, for the fundamental axial mode TEM_{00} and higher transversal modes TEM_{mn} with $1 \leq m+n \leq 3$ in the confocal resonator.*

4 Setup and equipment

We restrict the description to the most important parts of the kit which are essential for the experiments. Any additional information can be obtained from the original literature [3].

- With an output power of 2.5 mW, the **He-Ne laser** is classified as a class 3B product. The laser provides a temperature-dependent doublet emission line around 632.8 nm whose components are linearly polarized in perpendicular directions.

- Three pairs of **mirrors** are provided, two spherical sets with radii of curvature (ROC) of 75 mm and 100 mm, respectively; and one set of plane mirrors. The reflectivity of the mirrors is 96% for each set.

  Please, do not touch the mirror surfaces! The coatings are extremely damageable and expensive. Wear single-use gloves whenever you mount and replace the mirrors. For cleaning – even from dust etc. – special one-way lens tissues must be used. You should exercise yourself in "lens cleaning" with some dummy optics like a piece of window glass.

  In each mirror set, one of them is mounted on an axial **piezo translator**. The piezo ceramic actuator is driven by a maximum voltage amplitude of 150 V and provides an open loop sensitivity of ≈ 0.05 nm for 5 mV noise and a maximum force generation of 5500 N. The following list overviews other technical features of the device:

Type	max. stroke	length L	capacitance	stiffness	resonance
HPSt 500/15 – 8/7	13/8 µm	26 mm	140 nF	550 N/µm	30 kHz

- The piezo actuator may be controlled with respect to the amplitude, an offset and the frequency when moved back and forth according to a periodical delta voltage. Figure 7 illustrates the front panel of the **control unit PTC 1000**. The high voltage connector (BNC) for the piezo is located on the back, as well as the piezo voltage monitor and the trigger signal output.

- The output signal of the silicon **photo diode** (Siemens BPX 61) is amplified using the control unit PTC 1000. The device has an active area of $2.65 \times 2.65\,\mathrm{mm}^2$ which is sufficient to collect the unfocused laser light (FWHM $\sim$ 1 mm) without excessive losses. Its spectral range of sensitivity is given as $400\,\mathrm{nm} \leq \lambda \leq 1100\,\mathrm{nm}$, with a maximum around 850 nm.

  Although all measurements can be performed under daylight conditions, no direct sunlight or artificial room illumination should hit the photo diode in order to ensure an optimized contrast!

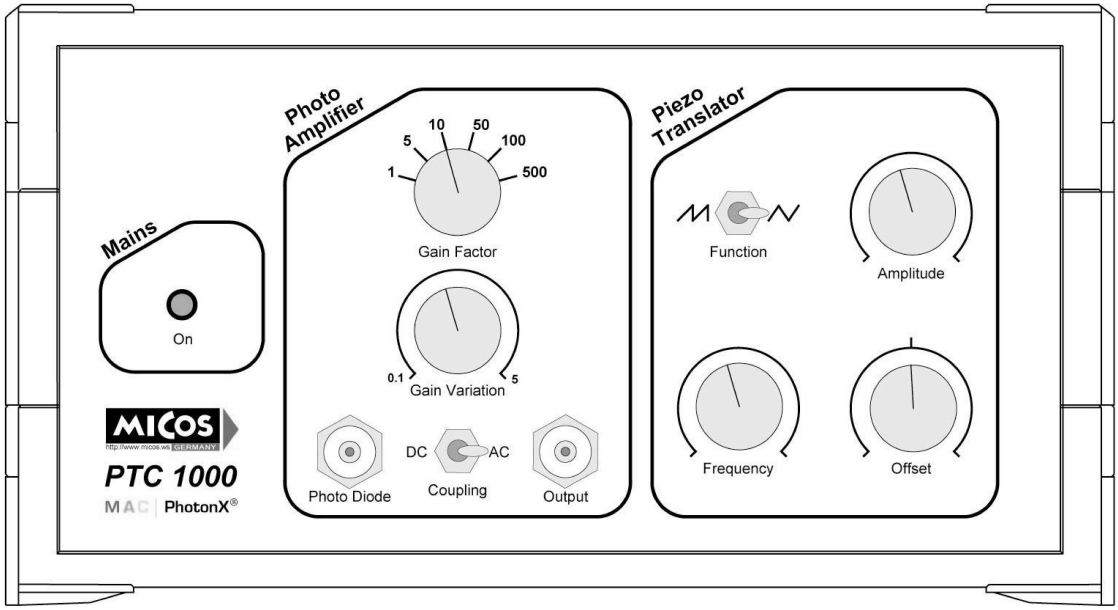

Figure 7: *Front panel of the control unit PTC 1000. In the "photo amplifier" unit, the gain may be varied within 0.1 and 2500. The frequency of the piezo triangle voltage can be set between 50 Hz and 100 Hz. Figure is taken from [3].*

- We use a Tektronix TDS 2012B **oscilloscope** with a bandwidth of 100 MHz. The amplified signal of the photo diode should be displayed on one channel, the second channel is reserved for the piezo triangle voltage. The oscilloscope is triggered externally by the control unit PTC 1000. The front panel is shown in Fig. 8.

  An USB Flash drive with a capacity ≤ 2 GB may be used for quick storage of screen shots in the .bmp format. The procedure is as follows:

  1. Put your USB memory stick into the "USB Flash Drive socket" and wait...
  2. Press the "SAVE/RECALL" button.
  3. Select Action "Save Image" and File format "BMP" on the screen.
  4. Select the function "Save TEKxxxx.BMP" on the screen and wait...

  Alternatively, you may use the oscilloscope software on the PC and "get the screen". This procedure is probably more comfortable. The complete printed manual of the instrument is available in the lab room [4]. Please, don't remove it from the lab.

- For the plane mirror arrangement, the laser beam should be expanded. One – adjustable – **divergent lens** with $f = -5$ mm and two focusing ones with $f = 20$ mm (achromatic) and $f = 150$ mm are available. The output of the resonator is focused onto the photo diode using a **convex lens** with $f = 60$ mm.

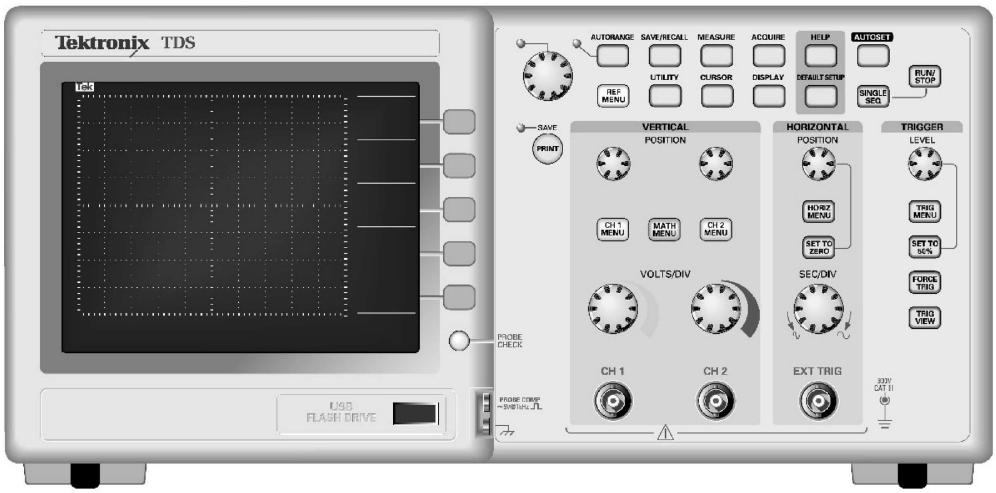

Figure 8: *Front panel of the TDS 2012B. An USB port for connection with a PC (remote control) is located on the back of the instrument. Figure is taken from [4].*

- A rotation stage equipped with a polarizer is used for measurements of the mode spectrum of the HeNe laser.

4.1 Practical procedure of the experiments

An appropriate adjustment of the resonator components along the optical axis is essential for successful measurements. In a first step, the confocal cavity with an ROC of 75 mm should be configured.

4.1.1 Confocal Arrangement for ROC = 75 mm

This standard setup may be adjusted quickly and is used for investigations of the mode spectrum of the laser and the determination of the piezo expansion. Figure 9 gives an overview of the configuration. For first explorations, the photo amplifier should be set to DC coupling, for a gain of about 50 (“Gain Variation” → center). It is reasonable to start with an ordinary triangle function for the piezo movement rather than the sawtooth profile. Choose an amplitude which is equivalent to a stroke near the maximum and medium values for frequency and offset. The recommended adjustment procedure is as follows (see Figure 10):

- Remove all tabs from the optical rail (1) except for the laser (2, 3). Align it as well as possible using the cross on the wall.
- Mount the tab with the photo diode on the rail and put the amplified (6) signal of the photo diode on one channel of the oscilloscope.

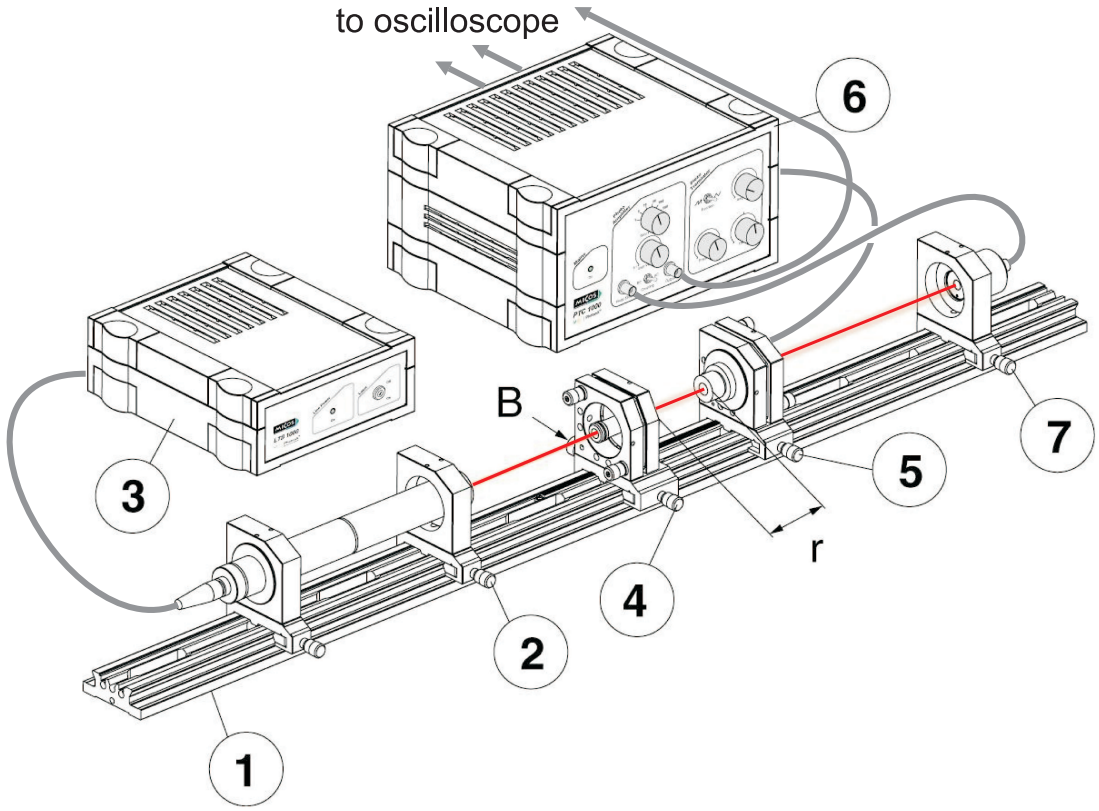

Figure 9: *Setup of the Fabry-Pérot resonator with spherical mirrors in the confocal mode: (1) optical rail – (2) laser with mounting – (3) laser power supply – (4) fixed resonator mirror – (5) piezo-driven resonator mirror – (6) control unit – (7) photo diode. Figure is adopted from [3].*

- Adjust both mirrors (ROC = 75 mm) *separately* using back reflections and concentric interference rings.
- The mirror distance should be coarsely set to the confocal condition $d = r$ using the scale on the optical rail.
- Switch on the piezo translator, using initially a medium amplitude and frequency. The piezo voltage is put on the second channel of the oscilloscope.
- Find an efficient method for fine tuning of the mirror distance until the interference contrast is maximized! For an optimized alignment, the finesse should approach the theoretical maximum.

Using the CURSOR function of the oscilloscope, the distance between the resonance peaks and their width (FWHM) are measured now. Store appropriate screen shots on your memory stick for reference. Measure the mirror distance including its estimated error!

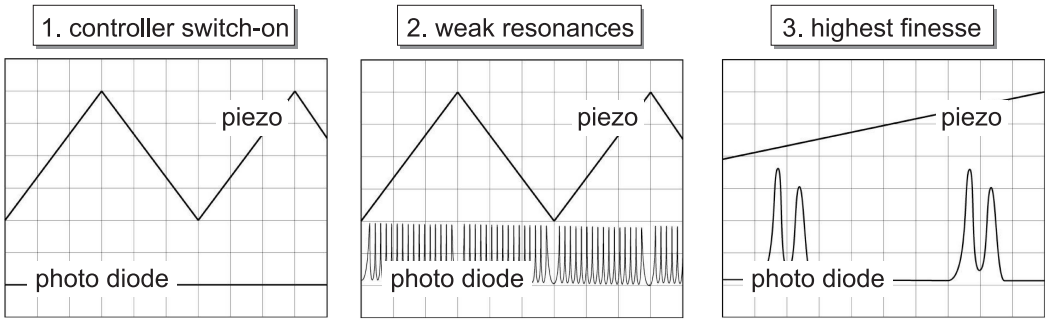

Figure 10: *Adjustment of the (confocal) setup. The amplitude of the resonances should be scaled down by reducing the gain at the control unit and / or the "volts / div" knob of the oscilloscope. Figures are adopted from [3].*

During the warm-up time of the laser tube, the mode spectrum of the HeNe emission around 632.8 nm varies. In particular, the relative intensities of the closely neighbored lines oscillate on time scales of several seconds. You should observe these variations until the equilibrium is reached. Now the *polarization* of the *final* peak intensities is measured for relevant angular positions $0° \leq \varphi < 360°$. Store the associated screen shots on your stick.

The piezo expansion rate is defined as the stroke in relation to the voltage difference and measured in units of [nm/V]. Check if it is independent of the piezo frequency and amplitude.

4.1.2 Stable Configurations for ROC = 100 mm

According to Section 3, the free spectral range (FSR) and the spectral resolution depend on the mirror distance d. Replace the spherical mirrors with $r = 75$ mm by those with an ROC of 100 mm and adjust the system again as described above. The distance between the resonance peaks and their width (FWHM) are measured again using the CURSOR. Store appropriate screen shots on your memory stick and estimate the real mirror distance using the scale on the optical bench.

The *stability* of an optical resonator depends on the geometry of the system. Aside from confocal arrangements, several other configurations allow stable operation. The general condition for a stable cavity is given as

$$0 \leq (1 - d/r_1) \cdot (1 - d/r_2) \leq 1 \tag{15}$$

for two mirrors with radii of curvature r_1 and r_2. This equation is illustrated in Fig. 11. For example, the concentric cavity is defined by $d = 2r$. Expand the mirror distance according to this condition and optimize the interference contrast. It might be helpful to use an additional focusing lens (e.g. $f = 60$ mm) in front of the photo diode. Record all required data and screen shots for the determination of the finesse as before.

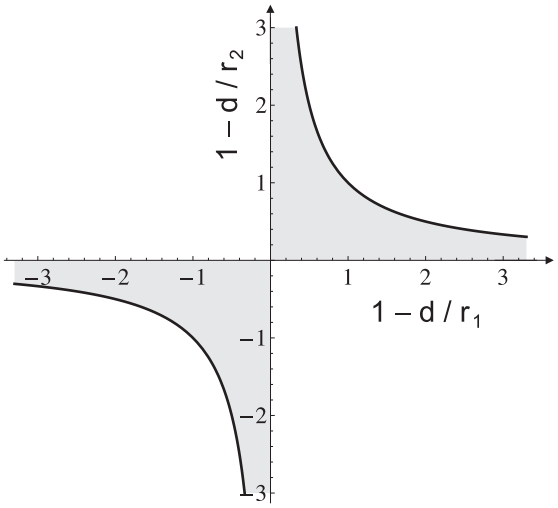

Figure 11: *Stability of optical resonators made of two mirrors with radii of curvature r_1 and r_2, separated by a distance d. The stable regions are gray underlaid and include the central point.*

4.1.3 Plane-Mirror Cavity

This experiment uses two plane resonator mirrors instead of spherical ones. An optimized detection of the interference rings requires a new experimental approach. Remove all optical mounts except for the laser.

- In a first step, the laser beam should be expanded with a two-lens telescope: It is recommended to use the $f = 150\,\text{mm}$ lens rather than the device with $f = 20\,\text{mm}$ in conjunction with the divergent lens ($f = -5\,\text{mm}$). The output beam must have a constant diameter, which is independent of the distance from the beam expander.
- Place the piezo-mounted mirror on the optical bench and adjust the back-reflected beam as accurate as possible. Switch off the control unit PTC 1000.
- Think about a reasonable mirror distance d. On the one hand, the sensitivity of the setup on misaligned mirror surfaces increases with the distance d. Thus, the adjustment is less challenging for a short mirror distance. On the other hand, the spectral resolution becomes better for large values of d.
- Place the second mirror on the bench and adjust it coarsely using back-reflections.
- Install the CMOS camera at the end of the optical bench and the convex lens ($f = 60\,\text{mm}$) in front of it – somewhat different from Fig. 12. Display the transmitted spot on the PC screen and center the CMOS camera to the optical axis.
- Think about an efficient “algorithm” for fine tuning of the cavity! Exploit the concentric fringe pattern which is shown on the PC screen (as on the left of Fig. 4).

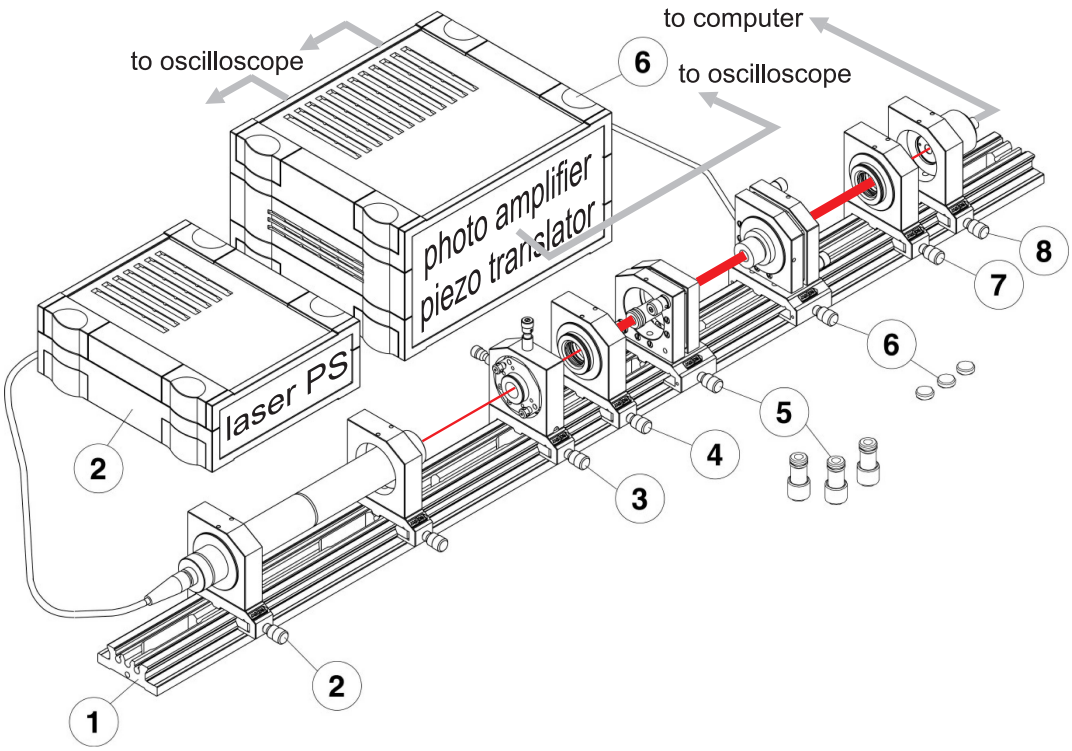

Figure 12: *Setup of the Fabry-Pérot resonator with plane mirrors: (1) optical rail – (2) laser with mounting and power supply – (3)+(4) beam expander – (5) fixed mirror – (6) piezo-driven mirror and control unit – (7) focusing lens – (8)* ***CMOS camera****. Figure is adopted from [3].*

- Set the polarizer into the laser beam and try to optimize the symmetry, sharpness and interference contrast of these so-called Haidinger rings. Exploit the polarizer for investigations of the mode spectrum, if applicable.
- Store at least one adequate image in the .bmp format on your memory stick – you may also record a cross section of the radial intensity distribution through the center of the ring pattern: The camera software offers an option for visualizing such one-dimensional cross sections in horizontal and / or vertical direction. You should get a screenshot by the combination $\langle ALT\ GR\rangle \bigoplus \langle PRINT\rangle$ and copy it from the clipboard into an empty work sheet of an appropriate software and store the file on your stick.
- Note your individual mirror separation d and estimate its uncertainty, i.e. $d \pm \Delta d$.

Download the CMOS camera manual [6] from the lab PC to your memory stick. You will need this reference for information on the sensor and pixel size of the camera. The model in use is called “DCC1545M".

5 Goals of the experimental work

In general, all calculations must be documented by **original measurement data**, i.e. tables, figures and appropriate print-outs or oscilloscope screen shots. Please, note important setup data like mirror distances and settings of the control unit PTC 1000 as well.

5.1 Characterization of confocal setup with ROC = 75 mm

Using the measured data for the peak width and their distance from each other, calculate the finesse as follows: Take an appropriate screen shot on the oscilloscope, similar to the right picture in Fig. 10. By means of the CURSOR function, measure the time distance $\delta\tau$ between two adjacent peaks of the same laser mode, corresponding to a phase shift $\Delta\phi = 2\pi$. In the same way, determine the full width at half maximum (FHWM) $\Delta\tau$ for at least one of them or – better – take the mean FHWM of both peaks. The ratio $\delta\tau/\Delta\tau$ yields the dimensionless finesse $\mathcal{F}$, though the latter one is defined by inverse units, i.e. frequencies. Why?

Give results for the free spectral range and the spectral resolution of your setup based on the *measured* mirror distance d in units of [Hz] and estimate their errors: The FSR $\delta\nu$ is obtained from (6) and its follow-up comments. Roughly approximated, its experimental error originates from the uncertainty of d and should be given as $\delta\nu = \langle\delta\nu\rangle \pm \Delta(\delta\nu)$. The spectral resolution is calculated now by means of (6) again, using the value for the finesse $\mathcal{F}$ from above. Its "± error" should be calculated in a similar way as for $\delta\nu$.

Compare your results with theoretical predictions from the mirror's reflectivity and their ROC: Use (5) and (6) once more, now for the nominal data provided by the manufacturer.

Determine the wavelength separation of the two adjacent laser emission lines and discuss their polarization properties: Note that you need to convert the directly measurable time difference from the oscilloscope into wavelengths. There is no linear relation as in case of the finesse! Why? The polarization features should be documented by a couple of printed screen shots for various angular positions of the polarizer.

Calculate the piezo expansion rate in units of [nm/V] from the oscilloscope screen shot: Consider what happens during piezo expansion: How are the observed resonance peaks of the Fabry-Pérot related to certain mechanical positions of the piezo? Use an oscilloscope display similar to the right in Fig. 10.

5.2 Characterization of confocal and concentric setup with ROC = 100 mm

Determine the finesse using the oscilloscope data. Calculate the free spectral range and the spectral resolution of this configuration as before and discuss your results: Obviously, the procedure is the same as for the "75 mm" case. Check if your data yield reasonable results.

Do the same for the concentric arrangement ($d = 2r$). Compare the performance with

the confocal case: Usually, the concentric resonator performs worse than the confocal one. Why? Be careful to get a regular resonance pattern as shown on the right in Fig. 10.

Copy the stability plot (Fig. 11) into your lab report and mark the corresponding points for the confocal and the concentric case. Calculate the stability criterion for all other combinations of mirrors used in this lab, i.e. the spherical ones with an ROC of 75 mm and 100 mm, respectively, and the plane mirrors ($r \to \infty$). In this way, you will obtain 6 possible resonator designs. Identify and discuss their stability in your plot.

5.3 Characterization of plane-mirror setup

Calculate the mirror distance and its standard deviation using the concentric ring system and compare your result with the directly measured value. Give the value of the excess ε: The procedure is described in Sect. 3, in particular by Fig. 4 and Eq. (10). At first, you should determine the diameters of at least three rings – don't confuse about the two laser modes – using a print-out of the CMOS image or by image-processing of its .bmp version.

For this purpose, the three-dimensional RGB data of the .bmp file must be first converted to one-dimensional gray-scale values. Depending on your software, this is done by a single command as in Mathematica for instance or alternatively in Photoshop or other software tools. Afterwards, the central row or column through the fringe pattern has to be extracted.

Plot your values for D_p^2 vs. the ring number p and add a linear least-squares fit to the data. If possible, take an appropriate software (Matlab, Mathematica, Maple,...) or an advanced scientific pocket calculator again for this task for the sake of accuracy. Note that an excess $\varepsilon < 0$ indicates an error in your analysis! So you should consider carefully the nature of the central intensity distribution, i.e. if it is indeed a single spot or a local minimum.

If you have recorded fringe patterns for both polarizations, you might even perform the procedure for those two adjacent modes and try to find their wavelength separation. Since the difference in the slope is very small, this operation works probably only for a sufficiently large number of detected rings and thus a small statistical uncertainty in the linear fit.

Calculate the interference order for this setup and deduce the FSR in units of [Hz]: As described by Eq. (4) and Fig. 5, the interference order is related to the wavelength λ and the mirror distance d. A modified version of this relation is valid for diffraction gratings, too. Why? If you want to measure the *absolute* wavelength of an unknown light source, would you either use a Fabry-Pérot resonator or that grating for spectroscopy?

Plot the radial cross section of the intensity distribution $I(r)$ and estimate the visibility as a function of the radius: There are two options for drawing $I(r)$. Either you may use the built-in function from the CMOS camera software and take a screen shot as described in Sect. 4.1.3. Alternatively, mathematical software tools extract the corresponding data row in the gray-level encoded matrix of the .bmp file. Once plotted, the peaks and the minima in between should be marked and measured both in radius and intensity. An example is illustrated in Fig. 13. The visibility is defined as $V(r) \equiv (I_{\max}(r) - I_{\min}(r))/(I_{\max}(r) + I_{\min}(r))$.

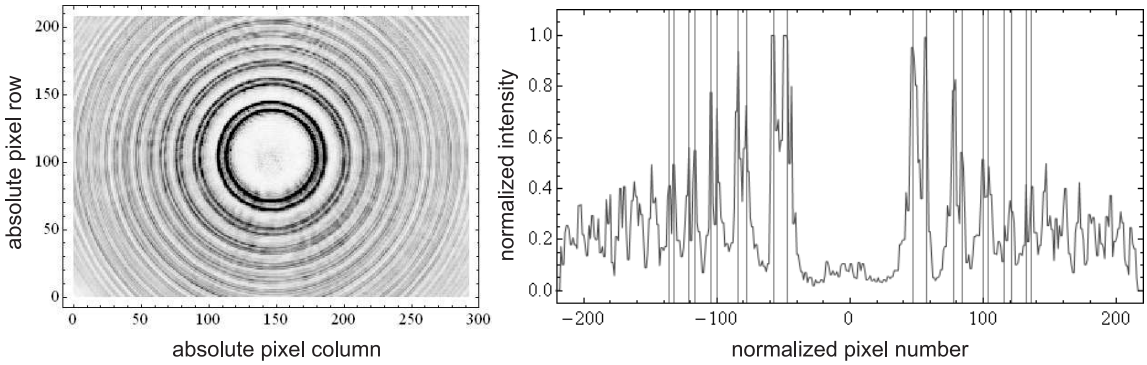

Figure 13: *Analysis of the plane-mirror fringe pattern. On the left, the .bmp pixel image is shown. On the right, a cross section through the center of the ring system reveals the peaks and minima.*

A Preliminary questions

Please, read up at home on the following keywords in common textbooks and / or the internet. You should be able to explain each of them with a few sentences and / or formulae:

HeNe laser, multiple-beam interference, (confocal) optical resonator, piezo actuator, coherence length, silicon photo diode, hyperfine structure spectrometry, dichroic filter, etalon, polarization of electromagnetic fields.

B Final questions

In addition, you should complete your lab report by solving the following problems. Their intention is to get an overview on the subject and a deeper understanding.

- In Sect. 3, the high spectral resolution of a Fabry-Pérot device was explained by multiple beam interference. Estimate the number of rays for an interferometer with a finesse $\mathcal{F}$. Compare your result with the number N of lines for a typical grating, whose resolving power in the m^{th} order is given as $\lambda/\Delta\lambda = mN$. How do Fabry-Pérot resonators achieve their spectral resolution?

- Give a reason why the free spectral range of a plane mirror cavity is always $c/(2d)$ whereas the FSR for confocal geometries may be just one half, i.e. $c/(4d)$ for pronounced off-axis beams. What is the FSR for concentric arrangements ($d = 2r$)?

- Calculate and plot the function $\mathcal{F}_t(\varrho)$ from Equation (11) for a mirror reflectivity of 96%. Why we don't use the beam expander for the confocal geometry?

- Lasers often use spherical mirrors in the confocal distance ($d = r$). Why is this arrangement so important?
- An important feature of optical resonators is their "stability". Scan the literature and / or the web in order to find out how the criterion from Section 4.1.2 is derived – at least in principle. Is it a "yes/no" criterion or may the stability be quantified?
- The plane mirror mode gives reason for simple investigations of the mirror surface quality. Unlike spherical ones, imperfect plane mirrors cause serious wavefront errors after multiple back and forth reflections, since even tiny phase shifts induced by small deviations from the ideal plane surface add up and smear out the interference contrast. The surface roughness is often measured in fractions of the wavelength, $\Delta h = \lambda/n$. Values $\Delta h < \lambda/100$ cannot be realized without an extraordinary technical effort. As a consequence, the finesse is usually limited to $\mathcal{F} \lesssim 50$, even for high reflecting mirrors. Fig. 14 compares both limits.

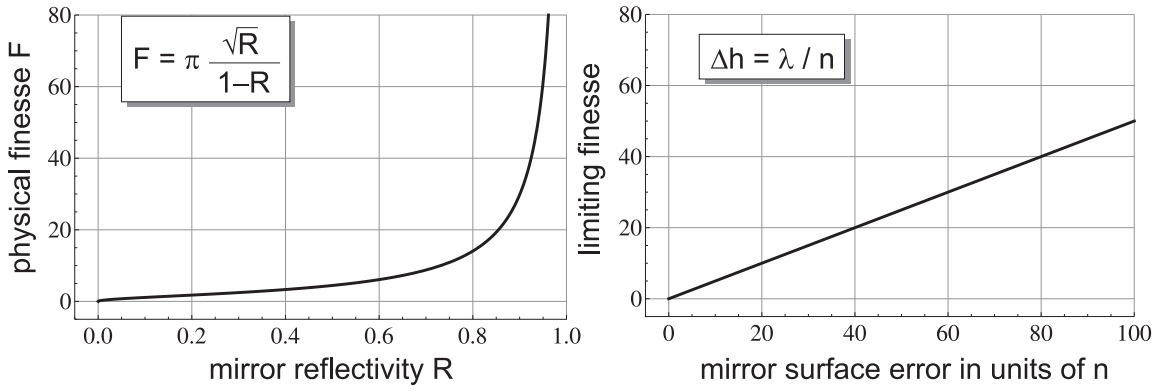

Figure 14: *The physical and technical finesse for plane mirrors. On the left, the reflection-based finesse $\mathcal{F}$ is shown. The technical limit is given in units of the wavelength fraction n (right).*

Give an explanation for the functional dependence on the right of Fig. 14. Following this elementary theory, you can estimate the required surface quality of the mirrors used in our lab for an optimized finesse near the theoretical limit.

- Reconsider the concentric ring pattern in the plane mirror arrangement. Should the mirror distance d be enlarged or diminished in order to contract the ring diameters?
- Following its definition in Sect. 5.3, the visibility V describes the interference contrast. Find the functional dependence $V(\mathcal{F})$ on the finesse.
- Why did we use the polarizer and a CMOS camera for the plane-mirror experiment? Based on the measured wavelength distance for the two-mode spectrum, estimate if they could have been resolved by *your* plane-mirror setup. Reason your statement!

C Preparation of the report

- Please keep the theory part as short as possible, about 1 – 2 pages with the most important concepts and equations. You should not just repeat the manual!
- Work through Sect. 5 step by step and try to answer all questions. Please include your answers to the preliminary (A) and final (B) questions, too.
- Describe in detail what you are measuring; i.e. all *original* plots and data must be provided. When you calculate your results, describe the way you found them (derivation of formulae).
- Make sure that all results are given with correct units. That is for instance to use [Hz] or $\left[\mathrm{s}^{-1}\right]$ for frequencies, not [s] or something else.
- Discuss your results, in particular in case of mismatching or contradictory results. If you were not able to do certain parts of the work program, please explain!

References

[1] `http://www.thorlabs.com`, "Scanning Fabry-Pérot Interferometers", 650 ff (2009).

[2] W. Demtröder, "Laser Spectroscopy Vol. 1: – Basic Principles", Springer-Verlag, Berlin/Heidelberg, 4th edition, 144-156 (2008).

[3] MICOS GmbH, "Laser Education Kit – CA-1140 Fabry Perot Resonator", miCos user manual, Eschbach (2009).

[4] Tektronix Inc., "TDS1000B and TDS2000B Series Digital Storage Oscilloscopes: User Manual", Beaverton, Oregon (2006).

[5] Dr. W. Luhs MEOS GmbH, "Fabry Perot Resonator", Eschbach (2003).

[6] Thorlabs GmbH, Operation Manual "High-Resolution USB2.0 CMOS and CCD Cameras", 85221 Dachau, Germany (2009).

Extra part. The knowledge presented here is not mandatory, but can improve your grade.

„Quantum Eraser“ with
MACH - ZEHNDER INTERFEROMETER

1. INTRODUCTION

The Mach-Zehnder interferometer is a device used to determine the relative phase shift variation between two collimated beams derived by splitting the light from a single source.
The light beam is first split into two parts by a beam splitter and then recombined by a second beam splitter. Depending on the relative phase acquired along the paths, the collimated beams will form constructive or destructive interference patterns on two screens placed after the second beam splitter.

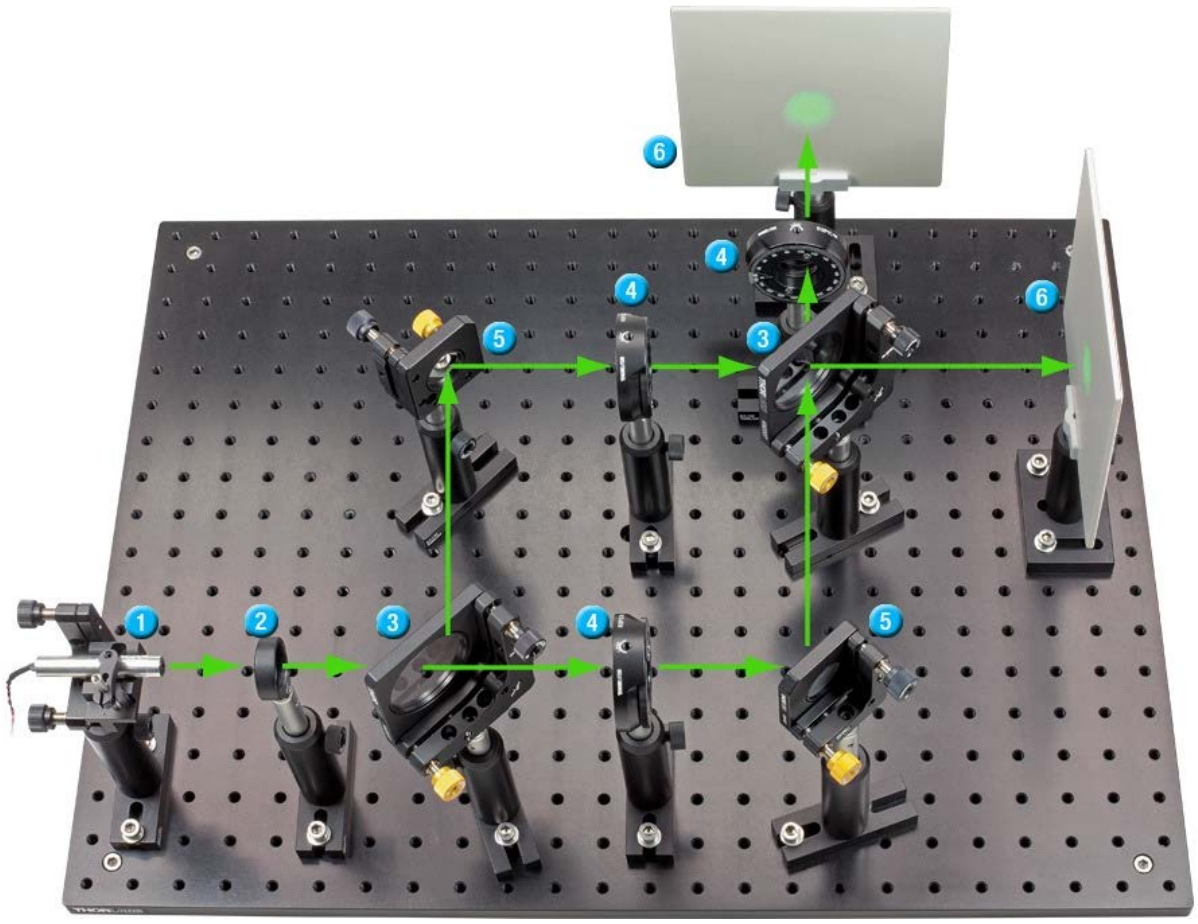

2. SETUP AND THEORETICAL BACKGROUND

The basic setup of a Mach-Zehnder interferometer is illustrated in Fig.1. It consists of a light source, tipically a laser, two beam splitters, two mirrors and two screens. The light beam is divided by the first beam splitter, giving origin to two different beams which travels “Path 1” and “Path 2”.

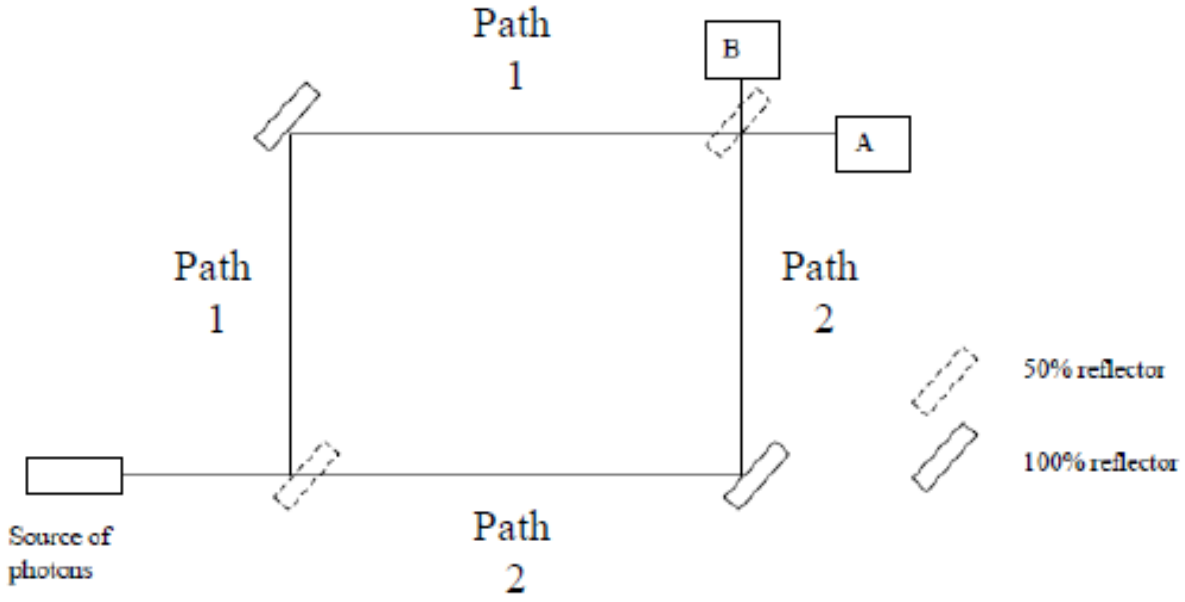

Fig. 1: Basic setup of a Mach-Zehnder interferometer [3].

At the Screen A it is possible to observe a bright spot (or, if we place a diverging lens between the laser and the first beam splitter, a interference ring pattern with a bright spot in the center), while the screen B remains dark (or, as before, it is illuminated with a interference ring pattern with a dark spot in the center). The situation is illustrated in Fig 2.

Fig. 2: Complementary interference ring patterns on the two screens A and B [1].

To understand the reason of this effect it is necessary to think about how the phase of a wave changes after reflection or refraction at the interface between two media.

Suppose to have a light beam which propagates in a medium with refraction index n_1 and reaches the interfaces with another medium with refraction index n_2. If we consider the reflected beam, two different cases have to be taken into account:

1) If $n_1 < n_2$, the phase will change by π.
2) If $n_1 > n_2$, the phase will not change.

Instead, the phase of the transmitted beam does not change, independently on the values of n_1 and n_2.

Being aware of that, we can explain the origin of the constructive and the destructive interference at the screens A and B, respectively.

Consider at first the formation of the interference ring pattern with a central dark spot at the screen B. The phase of the beam which travels along the path 1 changes by π after the reflection at the first beam splitter and by π after the reflection at the mirror. The reflection at the second beam splitter does not induce any additional change of phase, so this beam will reach the screen B with a total change of phase of 2π. The beam which travels along the path 2 undergoes instead to a total change of π (due to the reflection at the mirror) and so will interfere destructively with the other beam at the center of the screen B.

The situation at the screen A can be explained in a similar way. As before, the beam which travels along the path 1 reaches the screen A with a total change of phase of 2π. But in this case also the second beam undergoes to a total change of phase of 2π and this will result in a positive interference and a corresponding bright spot on the center of the screen.

Fig. 3: Disappearance of the interference patterns with two crossed polarizers along the paths 1 and 2 [1].

3. EFFECT OF THE BEAM POLARIZATION

The first objective of this experience is to investigate how the polarization state of the two beams affects the interference ring patterns on the two screens.

The starting configuration that we want to consider is the one with two parallel orientated polarizers, placed along path 1 and path 2, between the first beam splitter and the following mirrors.

What we should observe is that compared to the basic setup, nothing changes. This means that (placing as before one diverging lens in before the first beam splitter) on the screen B there will be an interference ring pattern with a central dark spot, while on the screen A the central spot will be bright.

If the two polarizers are instead perpendicularly, the interference patterns disappear and a bright spot appears on both screens, as it is illustrated in Fig 3.

Fig. 4: Recover of the interference pattern on one screen due to the third polarizer with intermediate polarization respect to the two crossed polarizers along the paths 1 and 2 [1].

When a third polarizer is placed in front of the screen B with intermediate polarization between the two crossed polarizers, the original interference pattern will appear again on the screen B (see Fig 4).

4. “WHICH PATH INFORMATION” IN QUANTUM PHYSICS

Until now we have considered a classical electromagnetism explanation in order to describe the formation of the interference ring patterns on the screens A and B. It is anyway possible to introduce a quantum mechanical description of the process, if we assume to reduce the intensity of the light so that the original beam consists only of single photons emitted with a measurable time separation between each other. Although we will not try to repeat the experience in such low-intensity regime, it is interesting to consider what could happen experimentally.

Consider at first the configuration in which the two polarizers are placed along the paths 1 and 2 parallel orientated. What we would observe are the previously described interference ring patters on the screens, with a dark or bright central spot on the screen B or A, respectively. From the classical physics point of view the result is not intuitive and is actually not predictable. To get a real comprehension of the effect it is necessary to describe it in the framework of quantum mechanics.

The quantum mechanical interpretation takes into account that when the two polarizers are parallel polarized, the paths 1 and 2 are undistinguishable. In quantum mechanics, when two states are not distinguishable, the physical system under interest (in this case the photon) is described as a superposition of both states. As long as the two paths are not distinguishable, we do not have any information about the actual path the photon travels along. The consequence is that when the photon reaches the screens, we have to treat it as a linear combination of two states: the photon which travels along the path 1 and the photon which travels along the path 2. The interference pattern that we observe is thus the result of the so called interference of the photon with "itself".

What we have presented in this section is a typical quantum mechanical effect: as long as the observer does not interact with the physical system, the last one is described as a superposition of different states (for example the energy levels of an atom). But as soon as we measure any physical observable of the system (that means, if we interact with it), the system will reduce itself to only one of these states.

5. QUESTIONS

After a description of the interferometer setup, the working principle and the experimental results, try to answer the following questions:

1) Why, in the frame of the classical electromagnetism, is the interference pattern on both screens destroyed when the two polarizers along the path 1 and 2 are crossed polarized? Why do you restore the original interference pattern by placing the third polarizer in front of the screen B with intermediate polarization?
2) Consider the situation of the single photon beam. Why do you observe a complementary interference ring pattern on the two screens (dark rings on one screen where you have bright rings on the other one)? Keeping in mind this experimental evidence, do you think that a single photon can be considered divisible?
3) What happens (again in the single photon beam regime) if the two polarizers along path 1 and path 2 are crossed polarized? Do you expect to observe an interference pattern?
4) Consider the situation introduced in the previous question. Why by placing the third polarizer with intermediate polarization in front of the screen B do you get again an

interference pattern? This polarizer is usually called “eraser” (from the verb “to erase”). Do you have any possible explanation for this expression?

References:

1) Please, copy the web-address to the command line http://www.thorlabs.de/thorcat/MTN/EDU-QE1_M-EnglishManual.pdf , “Quantum eraser”, 2013
2) J. D. Jackson, “Classical electrodynamics”, Wiley, 3th Edition (1998)
3) K.P. Zetie et al, Phys. Educ. 35(1) January 2000
4) R. Shankar, “Principles of Quantum Mechanics”, Plenum Press, 2th edition (1994)